INTERNATIONAL JOURNAL FOR NUMERICAL METHODS IN FLUIDS, VOL. 15, 1013–1024 (1992)

COMPUTATION OF INCOMPRESSIBLE VISCOUS FLOWS BY THE THIRD-ORDER UPWIND FINITE ELEMENT METHOD

NORIO KONDO

Department of Oceanic Architecture and Engineering, College of Science and Technology, Nihon University, 7-24-1, Narashinodai, Funabashi-shi, Chiba 274, Japan

NOBUYOSHI TOSAKA

Department of Mathematical Engineering, College of Industrial Technology, Nihon University, 1-2-1, Izumi-cho, Narashino-shi, Chiba 275, Japan

AND

TOSHIO NISHIMURA

Department of Oceanic Architecture and Engineering, College of Science and Technology, Nihon University, 7-24-1, Narashinodai, Funabashi-shi, Chiba 274, Japan

SUMMARY

A third-order upwind finite element scheme is presented for numerical solutions of incompressible viscous flow problems. In order to achieve the third-order upwind approximation for only the convection term in the Navier–Stokes equations, a simplified Petrov–Galerkin formulation in which a modified weighting function is expressed by the sum of a standard weighting function and its second and third spatial derivatives is employed. The mixed method is also employed in the formulation so that a discretization with high-order accuracy in space is carried out by the use of linear elements. Because a truncation error caused by the third-order upwind approximation is smaller than that of a first-order upwind scheme, it is expected that the third-order upwind scheme will greatly improve the numerical solutions of the Navier–Stokes equations. Numerical results in one and two dimensions are presented to illustrate the effectiveness of the proposed scheme.

KEY WORDS Third-order upwind scheme Finite element method Petrov–Galerkin formulation Mixed formulation

INTRODUCTION

In the computation of problems of convection-dominated flows, a scheme with a central difference approximation has given rise to solutions with spurious oscillations. On the other hand, upwind schemes[1–10] have been successful in obtaining solutions for convection-dominated flows and, as a consequence, have been recognized as a tool to avoid spurious oscillations in numerical solutions.

The early upwind schemes proposed by Christie *et al.*,[3] Heinrich *et al.*[4] and Zienkiewicz and Heinrich[5] are based on the Petrov–Galerkin formulation in which a modified weighting function is defined as a one-order higher function than a trial function. In these cases the modified weighting function is given as a standard weighting function, which leads to the Galerkin

0271–2091/92/211013–12$11.00 *Received March 1992*

formulation, plus a perturbation function. These upwind schemes have yielded satisfactory results for one-dimensional problems. Brooks and Hughes[6] proposed the streamline upwind/Petrov–Galerkin (SUPG) method with a discontinuous weighting function. The perturbation function used in the SUPG method is proportional to the first derivatives of the standard weighting function. Since the artificial viscous term added in the SUPG scheme acts only on the direction of flow, it is well known that the SUPG scheme is an overly effective scheme for the computation of multidimensional problems.

In this paper an upwind finite element scheme with third-order upwind approximation[1,2] is presented for solutions of the incompressible Navier–Stokes equations. The development of the upwind scheme is based on the simplified Petrov–Galerkin formulation and the mixed method. The perturbation function considered in the formulation is expressed by the sum of second and third spatial derivatives of the standard weighting function and it is also dependent only on the spatial discretization. The term of third derivatives plays the important role of producing artificial dissipation in combination with the Navier–Stokes equations. In our approach, since the order of spatial differentials in the modified weighting function is reduced by virtue of the mixed method, bilinear interpolation functions can be applied to unknown functions in the Petrov–Galerkin formulation when the finite element approximation is carried out. As is well known, the spatial accuracy of the Galerkin finite element scheme constructed on a uniform mesh is globally second-order. However, by adding the term of the second derivatives into the modified weighting function and employing the mixed method, we can get the finite element scheme[2] with a central approximation of fourth-order accuracy with respect to differential operators in space. Therefore we can easily make the finite element scheme with third-order upwinding such as in the case of the upwind finite difference approximation.[7,8]

Finally, numerical results for some test problems are presented. Computation of the Burgers equation, known as a one-dimensional model of a viscous fluid, is first carried out for $Re=5$, 100 and 1000. Next, numerical results of flow past a circular cylinder in a two-dimensional calculation are presented for $Re=100\,000$.

GOVERNING EQUATIONS

Let Ω be a bounded region in $\mathbb{R}^n$, where n is the number of space dimensions, and assume that Ω has a smooth boundary Γ. Let Γ_1 and Γ_2 be non-overlapping subsets of Γ and let n_i denote the outward normal vector on Γ.

Consider the incompressible Navier–Stokes equations written in the non-dimensional form

$$u_{i,t}+u_j u_{i,j}=\sigma_{ij,j}, \tag{1}$$

$$u_{i,i}=0. \tag{2}$$

In the above, u_i is the flow velocity and σ_{ij} is the total stress defined by

$$\sigma_{ij}=-p\delta_{ij}+\frac{1}{Re}(u_{i,j}+u_{j,i}), \tag{3}$$

where p is the pressure and Re denotes the Reynolds number.

The Dirichlet- and Neumann-type boundary conditions on Γ_1 and Γ_2 respectively are described as follows:

$$u_i=\hat{u}_i \quad \text{on } \Gamma_1, \tag{4}$$

$$\sigma_i=\sigma_{ij}n_j=\hat{\sigma}_i \quad \text{on } \Gamma_2, \tag{5}$$

where $\hat{u}_i$ and $\hat{\sigma}_i$ are prescribed functions of co-ordinates x_i and time t.

The initial condition is

$$u_i = \hat{u}_{0i} \quad \text{at } t = 0, \tag{6}$$

where $\hat{u}_{0i}$ is a given function of x_i.

UPWIND FINITE ELEMENT SCHEME

Petrov–Galerkin formulation

We now briefly present a third-order upwind finite element scheme[1,2] based on the Petrov–Galerkin formulation. Since a weak form of the Navier–Stokes equations is expressed in terms of the Petrov–Galerkin formulation, a modified weighting function $\bar{u}_i$ that is considered in the formulation is usually given by the form

$$\bar{u}_i = w_i + \tilde{w}_i, \tag{7}$$

where w_i is the continuous weighting function which leads to the Galerkin formulation and $\tilde{w}_i$ denotes a perturbation function of w_i. The weighting function for the continuity equation is denoted by q.

In general a physical domain considered in computation is divided into many non-uniform elements so that the detailed numerical results in the domain are adequately obtained. In this case, when the non-uniform mesh is used for making the finite element scheme, it is well known that the accuracy of spatial discretization of the scheme becomes lower-order. Therefore, if we introduce the following mapping transformations[11] with respect to space and time,

$$\xi_i = \xi_i(x_1, x_2, x_3, t), \qquad \tau = t, \tag{8}$$

we can propose a high-order-accurate finite element scheme in the transformed space such as in the case of the finite difference analysis.[7,8]

By the use of this transformation, the Petrov–Galerkin weighted residual equation of the Navier–Stokes equations can be written in the transformed space as

$$\int_{\bar{\Omega}} w_i(u_{i/\tau} + U_j u_{i/j}) J \, \mathrm{d}\bar{\Omega} + \int_{\bar{\Omega}} \xi_{k,j} w_{i/k} \sigma_{ij} J \, \mathrm{d}\bar{\Omega} + \int_{\bar{\Omega}} \tilde{w}_i(u_{i/\tau} + U_j u_{i/j} - \xi_{k,j}\sigma_{ij/k}) J \, \mathrm{d}\bar{\Omega} = \int_{\bar{\Gamma}} w_i \sigma_i I \, \mathrm{d}\bar{\Gamma}, \tag{9}$$

where $(\,)_{/\tau} = \partial/\partial\tau$, $(\,)_{/i} = \partial/\partial\xi_i$, $\mathrm{d}\Omega = J\mathrm{d}\bar{\Omega}$ and $\mathrm{d}\Gamma = I\mathrm{d}\bar{\Gamma}$, in which J and I denote the Jacobians respectively. The contravariant velocity U_i in (9) is defined by

$$U_i = \xi_{i,t} + \xi_{i,j} u_j. \tag{10}$$

Similarly, the weighted residual equation for the continuity equation becomes

$$\int_{\bar{\Omega}} \xi_{j,i} q u_{i/j} J \, \mathrm{d}\bar{\Omega} = 0. \tag{11}$$

Equation (9) is the exact formulation to construct the finite element scheme with upwinding. It is clear from (9) that an upwind technique is employed in all the terms in the Navier–Stokes equations (for the case of a one-dimensional steady advection–diffusion equation see Reference 2). In this case, because the upwind scheme developed is overly complex, it is desirable to adopt a simplified Petrov–Galerkin formulation in which the upwind technique is applied only to the convection term.

Then the simplified Petrov–Galerkin formulation that is used instead of (9) is written as

$$\int_{\bar{\Omega}} w_i u_{i/\tau} J \mathrm{d}\bar{\Omega} + \int_{\bar{\Omega}} (w_i + \tilde{w}_i) U_j u_{i/j} J \mathrm{d}\bar{\Omega} + \int_{\bar{\Omega}} \xi_{k,j} w_{i/k} \sigma_{ij} J \mathrm{d}\bar{\Omega} = \int_{\bar{\Gamma}} w_i \sigma_i I \mathrm{d}\bar{\Gamma}. \tag{12}$$

In the following subsection we shall propose a methodology which will develop a third-order upwind scheme by using (12), but centrally second-order accuracy for viscosity and pressure terms.

Mixed formulation

The perturbation function $\tilde{w}_i$ in (7) is defined by the form

$$\tilde{w}_i = -\tfrac{1}{3} \Delta\xi^2_{(j)} w_{i/(jj)} - \tfrac{1}{12} \alpha \Delta\xi^3_{(j)} \operatorname{sgn}(U_{(j)}) w_{i/(jjj)}, \tag{13}$$

where $\Delta\xi_i$ is the length of an element generated in the transformed domain and α is the parameter which is introduced to control the effect of artificial dissipation. For the index (j) with parentheses in the above expression, the summation convention is not employed. The range of the index (j) is defined as being equal to that of the repeated index j in the convection term of (12).

We use linear elements in order to interpolate all functions except for the pressure p and the weighting function q, and both p and q are assumed as constant on each element. Moreover, since we desire the development of the finite element scheme with third-order accuracy with respect to the convection term in (12), we have to employ the following auxiliary functions in order to obtain such a scheme:

$$\omega_i = J U_j u_{i/j}, \tag{14}$$

$$\phi_{i(j)} = \Delta\xi^2_{(j)} w_{i/(jj)}. \tag{15}$$

Substituting (3) and (13)–(15) into (12), we can get[1, 2]

$$\int_{\bar{\Omega}} w_i u_{i/\tau} J \mathrm{d}\bar{\Omega} + \int_{\bar{\Omega}} + (w_i \omega_i - \tfrac{1}{3} J U_j \phi_{i(j)} u_{i/j} - \tfrac{1}{12} \alpha \Delta\xi_{(j)} J |U_j| \phi_{i(j)/(j)} u_{i/j}) \mathrm{d}\bar{\Omega}$$
$$+ \int_{\bar{\Omega}} \frac{1}{Re} \xi_{k,j} w_{i/k} (\xi_{n,j} u_{i/n} + \xi_{n,i} u_{j/n}) J \mathrm{d}\bar{\Omega} - \int_{\bar{\Omega}} \xi_{j,i} w_{i/j} p J \mathrm{d}\bar{\Omega} = \int_{\bar{\Gamma}} w_i \sigma_i I \mathrm{d}\bar{\Gamma}. \tag{16}$$

On the other hand, denoting the weighting functions by $\bar{\omega}_{(i)}$ and $\bar{\phi}_{(ij)}$, the weighting residual equations of (14) and (15) are given as

$$\int_{\bar{\Omega}} \bar{\omega}_{(i)} \omega_i \mathrm{d}\bar{\Omega} = \int_{\bar{\Omega}} J U_j \bar{\omega}_{(i)} u_{i/j} \mathrm{d}\bar{\Omega}, \tag{17}$$

$$\int_{\bar{\Omega}} \bar{\phi}_{(ij)} \phi_{i(j)} \mathrm{d}\bar{\Omega} = -\int_{\bar{\Omega}} \Delta\xi^2_{(j)} \bar{\phi}_{(ij)/(j)} w_{i/(j)} \mathrm{d}\bar{\Omega} + \int_{\bar{\Gamma}} \Delta\xi^2_{(j)} \bar{\phi}_{(ij)} w_{i/(j)} n_{(j)} \mathrm{d}\bar{\Gamma}. \tag{18}$$

FINITE ELEMENT EQUATIONS

The finite element approximation of the weighted residual equations (16)–(18) leads to the following full discrete equations respectively:

$$\mathbf{W}^{\mathrm{T}} \mathbf{M} \mathbf{V}_{/\tau} + \mathbf{W}^{\mathrm{T}} \mathbf{B}_1 \boldsymbol{\Omega} - \boldsymbol{\Phi}^{\mathrm{T}} \mathbf{A}_3 \mathbf{V} - \boldsymbol{\Phi}^{\mathrm{T}} \mathbf{A}_4 \mathbf{V} + \mathbf{W}^{\mathrm{T}} \mathbf{K} \mathbf{V} - \mathbf{W}^{\mathrm{T}} \mathbf{C} \mathbf{P} = \mathbf{W}^{\mathrm{T}} \mathbf{F}, \tag{19}$$

$$\boldsymbol{\Omega} = \mathbf{M}_0^{-1} \mathbf{A}_1 \mathbf{V}, \tag{20}$$

$$\boldsymbol{\Phi} = -\mathbf{M}_0^{-1} \mathbf{B}_2 \mathbf{W}, \tag{21}$$

where $\mathbf{V}$, $\mathbf{W}$, $\mathbf{\Omega}$, $\mathbf{\Phi}$ and $\mathbf{P}$ are the vectors of nodal values of u_i, w_i, ω_i, $\phi_{i(j)}$ and p respectively, $\mathbf{F}$ is the force vector, $\mathbf{B}_1$, $\mathbf{B}_2$, $\mathbf{A}_1$, $\mathbf{A}_3$ and $\mathbf{A}_4$ are the matrices for the convection term, K is the matrix of the viscosity term, $\mathbf{C}$ is the gradient operator and $\mathbf{M}$ and $\mathbf{M}_0$ are lumped matrices.

Substituting (20) and (21) into (19), we can obtain the following upwind finite element equations for the Navier–Stokes equations:

$$\mathbf{M}\mathbf{V}_{/\tau}+(\mathbf{N}+\mathbf{K})\mathbf{V}-\mathbf{C}\mathbf{P}=\mathbf{F}, \tag{22}$$

where

$$\mathbf{N}=\mathbf{B}_1\mathbf{M}_0^{-1}\mathbf{A}_1+\mathbf{B}_2^{\mathrm{T}}\mathbf{M}_0^{-\mathrm{T}}\mathbf{A}_3+\mathbf{B}_2^{\mathrm{T}}\mathbf{M}_0^{-\mathrm{T}}\mathbf{A}_4. \tag{23}$$

The finite element equations for (11) are written as

$$\mathbf{C}^{\mathrm{T}}\mathbf{V}=\mathbf{0}. \tag{24}$$

In the finite element equation (22) the convection matrix $\mathbf{N}$ is constructed with the third-order upwind approximation[1,2] and the other matrices $\mathbf{K}$ and $\mathbf{C}$ are of central approximation with second-order accuracy.

NUMERICAL EXAMPLES

Problem of a discontinuity in one dimension

The Burgers equation in non-conservation form, known as a one-dimensional model of the Navier–Stokes equations,

$$u_{,t}+uu_{,x}=\frac{1}{Re}u_{,xx}, \tag{25}$$

is calculated in order to demonstrate the validity of the third-order upwind finite element scheme proposed in the previous section. In this case the pressure term $\mathbf{CP}$ in (22) is neglected, becuase in the Burgers equation the pressure p is assumed as a constant in the computational domain.

The initial conditions of this problem are given by

$$u(x,0)=1 \quad \text{for} \quad -x_{\max}\leqslant x\leqslant 0, \tag{26}$$

$$u(x,0)=0 \quad \text{for} \quad 0<x\leqslant x_{\max}. \tag{27}$$

The boundary conditions are

$$u(-x_{\max},t)=1, \tag{28}$$

$$u(x_{\max},t)=0. \tag{29}$$

On the other hand, equation (25) is equivalent to the conservation form

$$u_{,t}+F_{,x}=\frac{1}{Re}u_{,xx}, \tag{30}$$

where $F=u^2/2$. The exact solution[12] of (30) under the initial and boundary conditions (26)–(29) is given by

$$u=\int_{-\infty}^{\infty}\frac{x-\xi}{t}\mathrm{e}^{-0\cdot5ReG}\mathrm{d}\xi\Big/\int_{-\infty}^{\infty}\mathrm{e}^{-0\cdot5ReG}\mathrm{d}\xi, \tag{31}$$

where

$$G(\xi; x, t) = \int_0^{\xi} u(\bar{\xi}, 0)\mathrm{d}\bar{\xi} + \frac{0{\cdot}5(x-\xi)^2}{t}. \tag{32}$$

Computation of the Burgers equation (25) in non-conservation form is achieved by the Galerkin finite element (GFE) scheme, which is of the central approximation with second-order accuracy, the SUPG scheme and the third-order upwind finite element (TOUFE) scheme (22) with $\alpha = 1$, and then the numerical results are compared with the exact solution (31).

In these discrete schemes, when the solution vector $\mathbf{V}^n$ is given at a certain time level t_n, the solution vector $\mathbf{V}^{n+1}$ at a new time level $t_{n+1} = t_n + \Delta t$ is computed by the following two-stage Lax–Wendroff scheme:

$$\mathbf{V}^{n+1/2} = \mathbf{V}^n + \frac{\Delta t}{2}\mathbf{V}^n_{,t}, \tag{33}$$

$$\mathbf{V}^{n+1} = \mathbf{V}^n + \Delta t \mathbf{V}^{n+1/2}_{,t}. \tag{34}$$

Typical results for the schemes at $Re = 5$, 100 and 1000 are shown in Tables I–III respectively. For these calculations the initial velocity $u(0, 0)$ at $x = 0$ is particularly given as $u(0, 0) = 0{\cdot}5$ and a fine mesh is used so that the spurious oscillations do not appear in the numerical solutions.

In the computational results obtained by the SUPG and TOUFE schemes the velocity of the

Table I. Propagating shock solution at $t = 1$, $Re = 5$, $\Delta x = 0{\cdot}2$, $\Delta t = 0{\cdot}05$, $-2 \leqslant x \leqslant 2$

x / Scheme	−0·600	−0·400	−0·200	0·000	0·200	0·400	0·600	0·800	1·000	1·200	1·400	1·600
EXACT	0·989	0·973	0·937	0·868	0·753	0·591	0·409	0·247	0·132	0·063	0·027	0·011
GFE	0·992	0·978	0·945	0·876	0·755	0·585	0·398	0·238	0·127	0·062	0·028	0·012
SUPG	0·991	0·975	0·940	0·869	0·747	0·578	0·394	0·236	0·126	0·062	0·028	0·012
TOUFE	0·989	0·972	0·936	0·867	0·750	0·586	0·402	0·242	0·129	0·063	0·028	0·012

Table II. Propagating shock solution at $t = 1$, $Re = 100$, $\Delta x = 0{\cdot}01$, $\Delta t = 0{\cdot}001$, $-1 \leqslant x \leqslant 1$

x / Scheme	0·300	0·400	0·420	0·440	0·460	0·480	0·500	0·520	0·540	0·560	0·580	0·600
EXACT	1·000	0·993	0·982	0·953	0·881	0·731	0·500	0·269	0·119	0·047	0·018	0·007
GFE	1·000	0·995	0·985	0·958	0·887	0·732	0·493	0·262	0·116	0·047	0·018	0·007
SUPG	1·000	0·993	0·980	0·945	0·860	0·689	0·446	0·230	0·100	0·040	0·016	0·006
TOUFE	1·000	0·993	0·982	0·951	0·878	0·726	0·492	0·262	0·116	0·046	0·018	0·007

Table III. Propagating shock solution at $t = 1$, $Re = 1000$, $\Delta x = 0{\cdot}001$, $\Delta t = 0{\cdot}0001$, $-1 \leqslant x \leqslant 1$

x / Scheme	0·480	0·490	0·492	0·494	0·496	0·498	0·500	0·502	0·504	0·506	0·508	0·510
EXACT	1·000	0·993	0·982	0·953	0·881	0·731	0·500	0·269	0·119	0·047	0·018	0·007
GFE	1·000	0·995	0·985	0·958	0·887	0·732	0·493	0·262	0·116	0·047	0·018	0·007
SUPG	1·000	0·962	0·902	0·768	0·546	0·307	0·142	0·058	0·023	0·009	0·003	0·001
TOUFE	1·000	0·992	0·979	0·944	0·861	0·694	0·453	0·233	0·101	0·040	0·015	0·006

shock is slightly slower than the exact velocity. However, it is found that the solutions of the TOUFE scheme are better than those of the SUPG scheme.

The results for the third-order upwind finite element scheme are plotted with the exact solutions in Figures 1–3. The profiles of propagation of the shock are adequately captured.

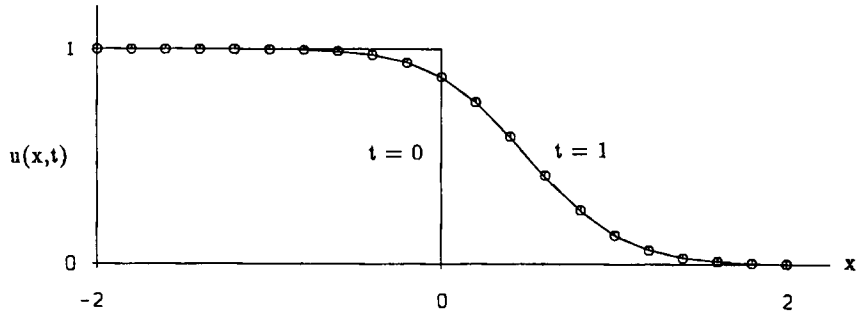

Figure 1. Propagating shock solution at $t=1$, $Re=5$, $\Delta x=0{\cdot}2$, $\Delta t=0{\cdot}05$, $-2\leqslant x\leqslant 2$: ○, exact; ——, third-order upwind finite element

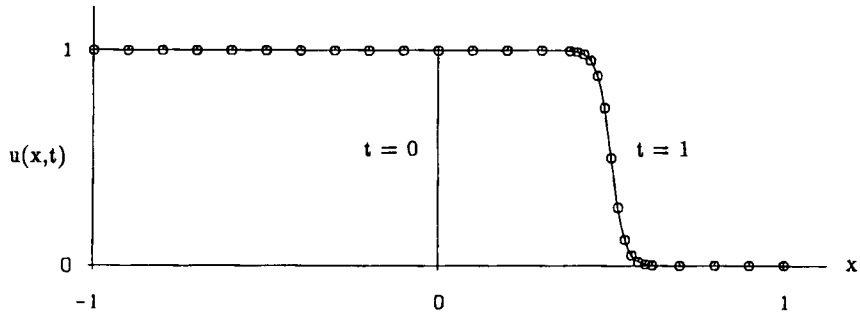

Figure 2. Propagating shock solution at $t=1$, $Re=100$, $\Delta x=0{\cdot}01$, $\Delta t=0{\cdot}001$, $-1\leqslant x\leqslant 1$: ○, exact; ——, third-order upwind finite element

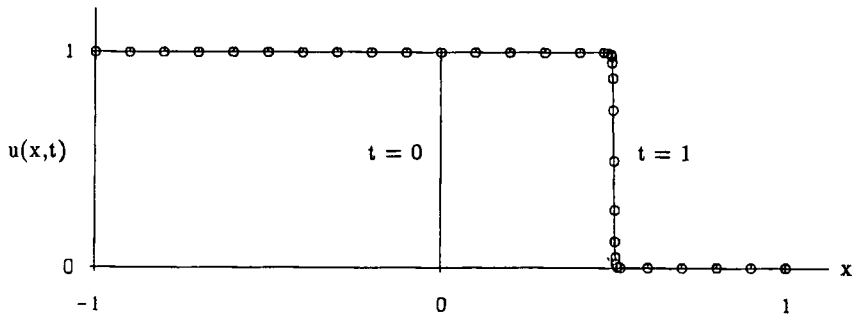

Figure 3. Propagating shock solution at $t=1$, $Re=1000$, $\Delta x=0{\cdot}001$, $\Delta t=0{\cdot}0001$, $-1\leqslant x\leqslant 1$: ○, exact; ——, third-order upwind finite element

Flow past a circular cylinder

Numerical results of flow past a circular cylinder at $Re = 100\,000$ are presented. The finite element mesh near the circular cylinder used in the calculation is shown in Figure 4. The total number of elements in the computational domain is 9000 and the total number of nodal points is 9220. The circumference of the circular cylinder is divided into 200 elements. The initial condition of flow is zero velocity everywhere. Time integration for (22) and (24) is achieved by a fractional step method.[13] In this calculation, we put $\alpha = 3$.

The velocity vectors and pressure contours for the fully developed Karman vortex are shown in Figures 5 and 6 respectively. The pressure distribution on the surface of the circular cylinder is shown in Figure 7. The mean drag coefficient C_D obtained by this calculation is approximately 1·30 and the Strouhal number St is approximately 0·192. Our results are in good agreement with the finite difference solutions[9] and experimental results.[14, 15]

CONCLUSIONS

In this paper we have presented the third-order upwind finite element scheme and have shown some numerical examples. Applying the Taylor series expansion to the artificial dissipation term written by the discrete expression, the artificial dissipation term can be rewritten by expression of the fourth derivatives of the flow velocity. As is clear from numerical results in one and two dimensions, our scheme gives satisfactory solutions. Therefore the proposed third-order upwind finite element scheme is overly effective in order to obtain the solutions in the range of high Reynolds numbers.

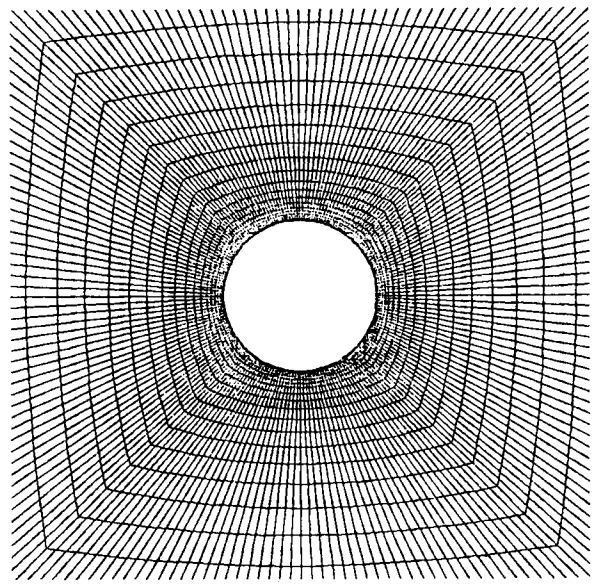

Figure 4. Finite element mesh near a circular cylinder

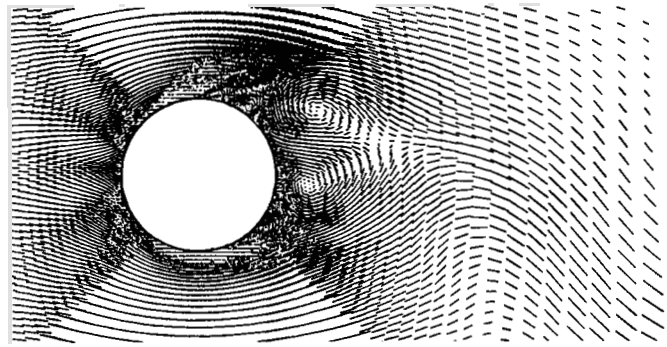

(a) t = 42

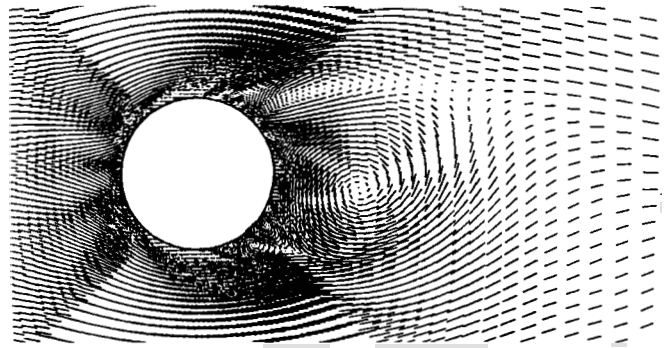

(b) t = 44

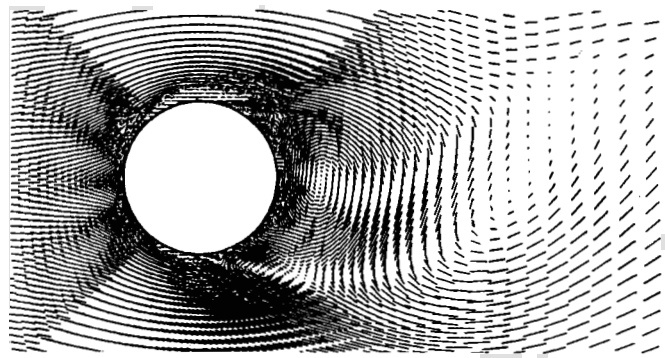

(c) t = 46

Figure 5. Computed velocity vector for $Re = 100\,000$

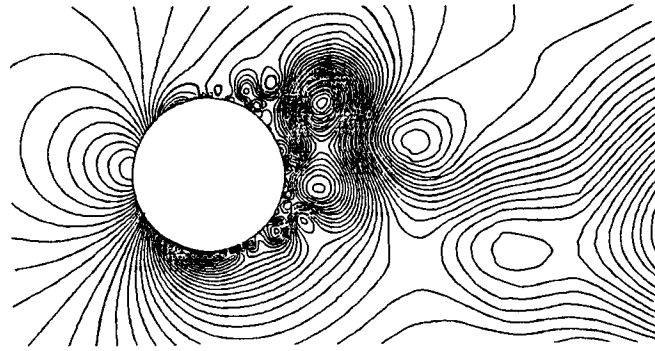

(a) t = 42

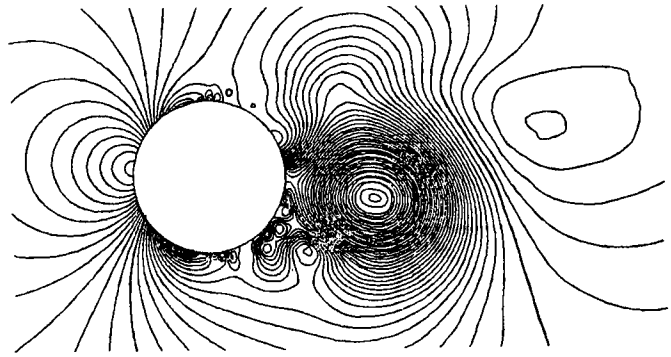

(b) t = 44

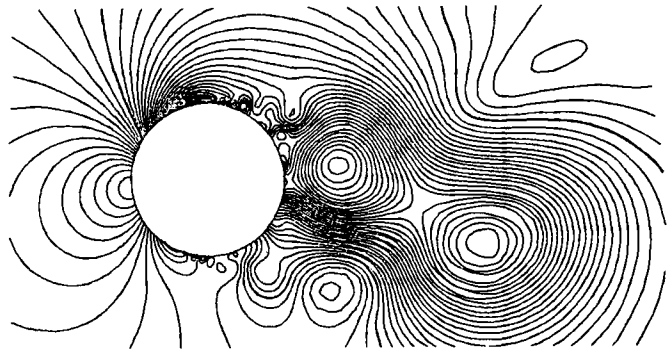

(c) t = 46

Figure 6. Computed pressure contours for $Re = 100\,000$

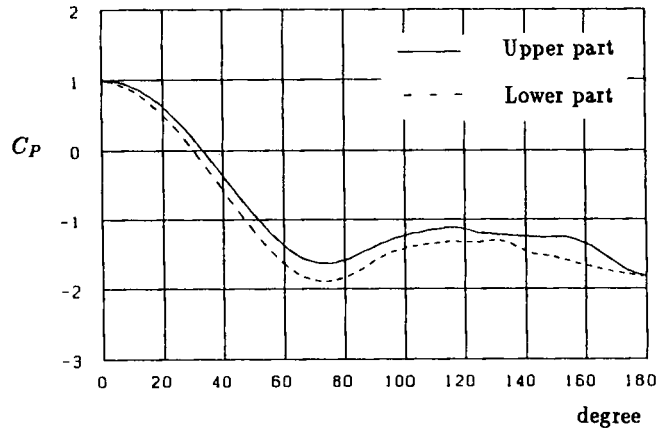

Figure 7. Pressure distribution on the circular cylinder for $Re = 100\,000$

APPENDIX

For simplicity we show the property of the convection matrix $\mathbf{N}$ in (22) by the use of the convection term $uu_{,x}$ in (25). In the case of the one-dimensional convection term, application of the procedure of Taylor series expansion to the discrete representation of $\mathbf{M}^{-1}\mathbf{NV}$ results in the following derivatives in non-conservation form and the truncation error:

$$\mathbf{M}^{-1}\mathbf{NV} \equiv Uu_{/\xi} + \tfrac{1}{12}\alpha\Delta\xi^3 |U| u_{/\xi\xi\xi\xi} + O(\Delta\xi^4). \tag{35}$$

In the above the second term on the right-hand side denotes the artificial dissipation.

REFERENCES

1. N. Kondo, N. Tosaka and T. Nishimura, 'Numerical simulation of viscous flows by the third-order upwind finite element method', *Theor. Appl. Mech.*, **39**, 237–250 (1990).
2. N. Kondo, N. Tosaka and T. Nishimura, 'Third-order upwind finite element formulations for incompressible viscous flow problems', *Comput. Methods Appl. Mech. Eng.*, **93**, 169–187 (1991).
3. L. Christie, D. F. Griffiths, A. R. Mitchell and O. C. Zienkiewicz, 'Finite element methods for second order differential equations with significant first derivative', *Int. j. numer. methods eng.*, **10**, 1389–1396 (1976).
4. J. C. Heinrich, P. S. Huyakorn, O. C. Zienkiewicz and A. R. Mitchell, 'An "upwind" finite element scheme for two-dimensional convective transport equations', *Int. j. numer. methods eng.*, **11**, 131–143 (1977).
5. O. C. Zienkiewicz and J. T. Heinrich, 'The finite element method and convective problems in fluid mechanics', in R. H. Gallagher *et al.* (eds), *Finite Elements in Fluids*, Vol. 3, Wiley, New York, 1978, pp. 1–22.
6. A. N. Brooks and J. T. R. Hughes, 'Streamline upwind/Petrov–Galerkin formulations for convective dominated flows with particular emphasis of the incompressible Navier–Stokes equations', *Comput. Methods Appl. Mech. Eng.*, **32**, 199–219 (1982).
7. B. P. Leonard, 'A survey of finite differences with upwinding for numerical modelling of the incompressible convective diffusion equation', in C. Taylor and K. Morgan (eds), *Computational Techniques in Transient and Turbulent Flow*, Pineridge, Swansea, 1981, pp. 1–35.
8. T. Kawamura and K. Kuwahara, 'Computation of high Reynolds number flow around a circular cylinder with surface roughness', *AIAA Paper 84-0340, AIAA 22nd Aerospace Science Meeting*, 1984.
9. T. Tamura and K. Kuwahara, 'Direct finite difference computation of turbulent flow around a circular cylinder', *Proc. Int. Symp. of Computational Fluid Dynamics*, 1989, pp. 701–706.
10. M. Tabata and S. Fujima, 'An upwind finite element scheme for high-Reynolds-number flows', *Int. j. numer. methods fluids*, **12**, 305–322 (1991).

11. F. Thompson, Z. U. A. Marsi and C. W. Mastin, *Numerical Grid Generation, Foundation and Application*, North-Holland, Amsterdam, 1985.
12. C. A. J. Fletcher, *Computational Techniques for Fluid Dynamics*, Vol. 1, Springer, Berlin, 1988.
13. J. Donea, S. Giuliani, H. Laval and L. Quartapelle, 'Finite element solution of the unsteady Navier–Stokes equations by a fractional step method', *Comput. Methods Appl. Mech. Eng.*, **30**, 53–73 (1982).
14. B. Cantwell and D. Coles, 'An experimental study of entrainment and transport in the turbulent near wake of a circular cylinder', *J. Fluid Mech.*, **136**, 321–374 (1983).
15. H. Schlichting, *Boundary-layer Theory*, 7th edn, McGraw-Hill, New York, 1979.